

Morphological and Quantitative Evaluation of Emphysema in Chronic Obstructive Pulmonary Disease Patients: A Comparative Study of MRI With CT

David J. Roach PhD,^{1,2} Yannick Crémillieux PhD,³ Suraj D. Serai PhD,⁴
Robert P. Thomen MS,^{1,5} Hui Wang PhD,⁶ Yuanshu Zou PhD,⁷
Rhonda D. Szczesniak PhD,^{2,7} Sadia Benzaquen MD,⁸ and
Jason C. Woods PhD^{1,2,4*}

Purpose: To further validate the ability of ultrashort echo-time (UTE) magnetic resonance imaging (MRI) in quantifying lung density in patients diagnosed with chronic obstructive pulmonary disease (COPD) and to develop an MRI-based emphysema index (EI).

Materials and Methods: Ten subjects clinically diagnosed with COPD (5M/5F, age 62.6 ± 8.5 years) and ten healthy subjects (2M/8F, age 48.9 ± 19.2 years) were imaged via UTE MRI at 3T (4 mm slices, 1.39×1.39 mm² pixels). Chest computed tomography (CT) images (generally 5 mm slices, $\approx 0.55 \times 0.55$ mm² pixels), acquired retrospectively, were compared to UTE MRI. CT lung densities, MR lung-signal density, and EI were quantified from both CT and UTE MR images via a quantitative automated analysis and compared to the percent predicted forced expiratory volume in 1 second (FEV₁% predicted).

Results: EI quantified in controls via CT and UTE MRI was $0.23 \pm 0.78\%$ and $2.40 \pm 1.50\%$, respectively; in COPD subjects it was $13.3 \pm 14.9\%$ ($P = 0.021$) and $12.0 \pm 9.8\%$ ($P = 0.013$), respectively. Bland–Altman determined the mean differences and 95% limits of agreement for COPD subjects and healthy controls were 0.06 (12.50 to -12.38). Strong correlation ($R^2 = 0.79$, $P < 0.0001$) existed between EIs quantified from both CT and UTE MRI. There was a slightly higher correlation between FEV₁% predicted and the UTE MRI EI ($R^2 = 0.65$, $P < 0.0001$) compared to CT EI ($R^2 = 0.49$, $P < 0.0001$).

Conclusion: Our results demonstrate a significant positive correlation between lung density and EI assessed with CT and MRI. Furthermore, UTE MRI exhibits its potential as a diagnostic alternative to CT for assessing the extent and the severity of emphysema, particularly for longitudinal studies.

J. MAGN. RESON. IMAGING 2016;44:1656–1663.

Chronic obstructive pulmonary disease (COPD) is a heterogeneous disease that affects the airways, parenchyma, and vasculature and is characterized by irreversible airflow obstruction resulting from both emphysema and chronic bronchitis. It is a leading cause of morbidity and

mortality worldwide.^{1,2} Computed tomography (CT) is the standard imaging technique for assessing lung anatomy and for grading and staging of emphysema in patients. Although advances in CT scanners permit greater volume coverage with a higher resolution and lower radiation dosage,

View this article online at wileyonlinelibrary.com. DOI: 10.1002/jmri.25309

Received Feb 4, 2016, Accepted for publication Apr 27, 2016.

*Address reprint requests to: J.C.W., Center for Pulmonary Imaging Research, Cincinnati Children's Hospital Medical Center, 3333 Burnet Ave., Cincinnati, OH 45229. E-mail: Jason.Woods@cchmc.org

From the ¹Center for Pulmonary Imaging Research, Cincinnati Children's Hospital Medical Center, Cincinnati, Ohio, USA; ²Pulmonary Medicine, Cincinnati Children's Hospital, Cincinnati, Ohio, USA; ³Centre de Résonance Magnétique des Systèmes Biologiques, Centre National de la Recherche Scientifique, Université de Bordeaux, Bordeaux, France; ⁴Radiology Department Cincinnati Children's Hospital, Cincinnati, Ohio, USA; ⁵Department of Physics, Washington University in St. Louis, St. Louis, Missouri, USA; ⁶Philips Healthcare, Cleveland, Ohio, USA; ⁷Biostatistics and Epidemiology, Cincinnati Children's Hospital, Cincinnati, Ohio, USA; and ⁸University of Cincinnati College of Medicine, Cincinnati, Ohio, USA

Additional Supporting Information may be found in the online version of this article.

ionizing radiation is still a concern for longitudinal follow-up and clinical studies.³

Compared to CT, magnetic resonance imaging (MRI) is advantageous in that it does not involve ionizing radiation, which mitigates the risk of radiation-induced mortality, and lends itself to serial and longitudinal scanning.⁴ However, pulmonary imaging via MR is intrinsically difficult due to the low proton density of the lungs and physiological motion caused by respiration and cardiac motion. Additionally, multiple air–tissue interfaces within the lungs (alveoli) produce local magnetic-susceptibility gradients, leading to an exceedingly short effective transverse relaxation time (T_2^*) of the lung parenchyma (≈ 0.7 – 0.8 msec at 3T).^{5,6} Despite these inherent difficulties, advances have been made in evaluating structural and functional pulmonary information with the development of faster and more sensitive ^1H MRI techniques such as ultrashort echo-time (UTE) and Fourier decomposition methods.^{7–11} Structural lung information can be assessed through radial or spiral k -space acquisition, reducing the echo-time (TE) to as low as 100 microseconds and minimizing the parenchyma signal decay due to short T_2^* .¹²

Recent pulmonary UTE MRI studies have demonstrated this technique's ability at quantifying parenchymal lung-signal as a function of lung inflation level and/or the presence of emphysema in human subjects and murine models.^{13–19} Notably, one study demonstrated that the signal of the lung parenchyma can be used to assess human lung density with sensitivity to lung inflation and gravitational dependence.¹³ A more recent study focused on human COPD subjects and demonstrated that UTE MRI lung-signal intensity correlated with CT lung density measurements and pulmonary function test (PFT) results.¹⁴ A separate study demonstrated that T_2^* maps correlated with CT measurements of smoking-related pulmonary function, providing the ability to differentiate between the clinical stages of COPD.¹⁵ Additionally, several pulmonary UTE MRI studies using murine models demonstrated this technique's ability to assess the change in signal intensity as a function of lung inflation level,¹⁶ the reduced signal intensity of emphysematous lung compared to healthy lung,¹⁷ and the progression of emphysema.¹⁸

Fourier decomposition, a noncontrast and nongating technique, has been utilized in measuring functional lung information such as regional pulmonary ventilation and perfusion but without quantification until recently.^{19–21} This technique has demonstrated its clinically acceptable reproducibility and has potential for respiratory disease follow-up. Inhaled hyperpolarized noble gases, such as ^3He and ^{129}Xe , have been utilized as MRI contrast media for measuring pulmonary functional biomarkers, which include lung ventilation, quantification of airway microstructures, and gas exchange.^{22–25} However, the high cost and shortage of ^3He ,

historically lower polarization in ^{129}Xe , along with the need for polarizers and specialized hardware limit this technique to certain research institutions.²⁶ Overall, pulmonary imaging via MRI is continuously evolving and gaining footing as a possible imaging surrogate for CT.

In our present work we imaged adult subjects clinically diagnosed with COPD and age-matched healthy controls via UTE MRI. The purpose of this study was to further validate a UTE MRI protocol in assessing emphysematous lung in COPD patients and demonstrate its potential as an alternative imaging modality to CT. Importantly, we sought to develop a UTE MRI emphysema index (EI) comparable to the well-validated CT emphysema index.^{27–29} A validated MRI-based EI could potentially lead to increased surveillance of emphysema progression in COPD patients without increased exposure to ionizing radiation.

Materials and Methods

Patient Study

This study was approved by the Institutional Review Board at Cincinnati Children's Hospital Medical Center (IRB approval number 2013-4847) and the University of Cincinnati. Informed consent was obtained from all participants and the subjects were imaged from July 26, 2013 to April 22, 2015. Ten medically stable subjects with clinically diagnosed COPD, as per diagnosis and CT evidence of emphysema (5M/5F, mean \pm SD age 62.6 ± 8.5 years; range: 51–77 years) were recruited.³⁰ Eight healthy subjects (2M/6F, age 54.0 ± 18.1 years; range: 28–78 years), with clinically indicated thoracic CT with negative pathology and no current history of smoking within 3 months or recent pulmonary infection were enrolled and imaged via UTE MRI. Two additional control group sets were added to this analysis: 10 healthy subjects (3M/7F, age 47.3 ± 6.34 years; range: 41–62 years) with existing CT and percent predicted forced expiratory volume in 1 second (FEV₁% predicted), and two healthy subjects (2F, age 28.5 ± 0.71 years; range: 28–29 years) with UTE MRI and FEV₁% predicted.

CT Examination

Each subject's most recent clinically indicated chest CT was reviewed; the average time between CT and MRI of all subjects was 9.4 ± 20 months. The CT images used for evaluation were acquired at each subject's corresponding medical center. Inspiratory CT data from various manufacturers were used: Siemens (Erlangen, Germany, Sensation 64, Somatom Definition), Philips (Best, Netherlands, iCT 256), Toshiba (Tustin, CA, Aquilion), GE (Milwaukee, WI, LightSpeed VCT). CT images were acquired with the following general parameters: coached breath-hold at inspiration, axial orientation, slice thickness ranged from 0.7 to 5 mm, a medium convolution kernel (B31f, B30f, FC07, or Standard), and an in-plane resolution which varied from $0.55 \times 0.55 \text{ mm}^2$ to $0.78 \times 0.78 \text{ mm}^2$. Expiratory CT images were not uniformly acquired and hence were excluded from analysis.

Clinical Testing

If subjects had no recent clinically acquired PFTs within 6 months of MRI, subjects performed a same-day spirometry test using a

handheld portable spirometer (Koko, nSpire, Longmont, CO) according to ATS/ERS guidelines.

¹H UTE MRI Protocols

All MRIs were performed with a commercially available 3T MR unit (Achieva; Philips Healthcare) with a 32-channel cardiac phased-array coil. Axial quantitative lung images were acquired during free breathing using an ultrashort-TE 3D stack-of-stars sequence, which entails 2D radial sampling in the transverse plane and Cartesian encoding along the longitudinal plane. The following parameters of the UTE sequence acquisition were: TR/TE 2.7/0.17 msec; flip angle (FA) 5°; selective radiofrequency (RF) pulse; matrix size 288 × 288; field of view (FOV) 400 × 400 mm; slice thickness 4.0 mm; and voxel size 1.39 × 1.39 × 4.0 mm. Subjects were asked to breathe normally at a tidal volume during image acquisition. An echo navigator was positioned on the lung–liver interface and image acquisition was gated during expiration to capture lung-signal at functional residual capacity (FRC). UTE MR images were acquired during free breathing with RF excitation and signal acquisition limited to a gated acquisition window to yield heavily spin-density weighted lung images. Regional saturation technique (REST) slabs were placed above and below the imaging slab to minimize aliasing artifacts. Two hundred lines of *k*-space were acquired per gating window and scan time ranged from 12–15 minutes, depending on the breathing rate of the subject. The total time in the scanner including patient positioning, localizer scan, and UTE scan was ~20 minutes. Scan time restraints limited the number of slices acquired to ~40, which captured the majority of the lungs but sometimes clipped the most apical and basal sections of the lungs (<20% of the lung volume).

Automated Quantitative Analysis

Lung segmentation was performed using a commercially available software program (Amira, Hillsboro, OR). For CT images, both lungs were individually segmented from the body and large lung vessels using a threshold of <-500 Hounsfield units (HU). The average HU of the left and right lung (<HU>) was measured along with the respective lung volumes (V_L), which were quantified by summing the voxels within the lungs. Based on the <HU> of each lung, mean lung densities (<ρ_{CT}>) of both left and right lungs were determined via Eq. (1):

$$\langle \rho_{CT} \rangle = \left(\frac{1000 + \langle HU \rangle}{1000} \right) \quad (1)$$

Low attenuation areas or emphysematous lung was defined as lung with an x-ray attenuation value at inspiration of <-950 HU and was segmented from healthy lung tissue at total lung capacity.^{27–29} An emphysema index (EI),² defined as the percentage or volume-fraction of emphysematous lung volume (EV_L) over the total lung volume (TV_L), was determined for each subject.

$$EI = \frac{EV_L}{TV_L} \times 100 \quad (2)$$

In the automated quantitative analysis of the UTE MR images, all but the two most basal and apical slices were used due to signal dropoff caused by REST slabs. For UTE MR images, the lungs

were segmented from the soft body tissue and vessels using an initial threshold value of <70% of the mean thoracic soft-tissue signal with user oversight. Using this threshold value the large lung vasculature was excluded from our analysis of the lung. A threshold value of <10% of the mean thoracic soft-tissue signal was used to segment the lower-signal regions from healthy lung in our proton-density-weighted regime. While this threshold value was chosen empirically to maximize the contrast of emphysematous lung between the COPD subjects and controls, we note that it corresponds to an approximate CT value of -900 HU, which is close to a reasonable emphysema density threshold for functional residual capacity (where the MRI is obtained). Additional threshold values were investigated and summary of results are supplied in the online supplement. The mean lung-signal intensity, which is defined as S_L, was normalized to the mean thoracic soft-tissue signal, S_M, to quantify relative lung-signal densities of both the right and left lung, <ρ_{MRI}>:

$$\langle \rho_{MRI} \rangle = \frac{S_L}{S_M} \times 100 \quad (3)$$

The EV_L and TV_L were determined for each subject so that an MRI emphysema index similar to the CT emphysema index, as defined above in Eq. (2), could be quantified. Additionally, the signal-to-noise ratio (SNR) was computed as the ratio of the mean lung-signal intensity divided by the standard deviation of the image background signal intensity. In our small-flip-angle (proton-density-weighted) regime UTE MR images are still slightly T₁- and T₂-weighted, so <ρ_{MRI}> represents signal density rather than mass density.

Regional Analysis

A regional lung analysis of the MR images was performed to assess the robustness of our automated quantitative analysis in utilizing the mean thoracic soft-body tissue to normalize the lung-signal in quantifying lung-signal density. Four bronchopulmonary slices were chosen at the level of the aortic arch, carina, a slice above the top of the diaphragm, and an intermediate slice equal distance between carina and top of the diaphragm. A total of 12 regions of interest (ROIs) (of similar area) were chosen per bronchopulmonary slice. ROIs were placed in both the anterior, mid, and posterior portions of the left and right lung, capturing few to no vessels, along with six ROIs placed in muscle juxtaposed to the respective lung ROI. Mean surface area of the ROIs was 305 mm² ± 22 (SD). Each lung ROI was then normalized to its corresponding muscle ROI to determine the regional relative lung-signal density. For CT images a similar regional lung analysis was performed. A total of six ROIs (of similar area) were drawn per bronchopulmonary axial slice. ROIs were placed in both the anterior, mid, and posterior portions of the left and right lungs, and captured few to no vessels. The mean HU of each ROI was measured to assess regional lung densities and compared to regional MR lung-signal densities.

Statistical Analysis

Lung densities and volume percentages of emphysematous lung (EI) are each summarized as mean ± SD. Comparison of these percentages and lung densities quantified for both COPD subjects and healthy controls via CT and UTE MRI was performed using a non-parametric unpaired *t*-test. *P*-values less than 0.05 (two-sided) were

TABLE 1. Subject Demographics

Group	Height (cm)	Weight (kg)	BMI	Sex	Age (Y)
COPD	168.8 ± 10.6	66.4 ± 12.5	23.4 ± 4.5	5M/5F	62.6 ± 8.5
ControlGroup1 (<i>t</i> -test vs. COPD)	163.8 ± 7.1 (<i>P</i> = 0.26)	75.8 ± 10.0 (<i>P</i> = 0.09)	28.5 ± 3.8 (<i>P</i> = 0.02)	2M/6F	54.0 ± 18.1 (<i>P</i> = 0.24)
ControlGroup2 – MRI Only (<i>t</i> -test vs. COPD)	160.5 ± 0.7 (<i>P</i> = 0.04)	70.4 ± 14.0 (0.76)	27.3 ± 5.2 (<i>P</i> = 0.43)	2F	28.5 ± 0.7 (<i>P</i> < 0.001)
ControlGroup3 – CT Only (<i>t</i> -test vs. COPD)	163.6 ± 25.2 (<i>P</i> = 0.53)	80.7 ± 14.9 (<i>P</i> = 0.03)	29.1 ± 1.3 (<i>P</i> = 0.06)	3M/7F	47.3 ± 6.3 (<i>P</i> < 0.001)
All Controls (<i>t</i> -test vs. COPD)	163.3 ± 18.3 (<i>P</i> = 0.32)	77.7 ± 12.8 (<i>P</i> = 0.03)	30.5 ± 11.3 (<i>P</i> = 0.02)	5M/15F	48.1 ± 14.0 (<i>P</i> = 0.002)

ControlGroup1 has CT and UTE MRI, ControlGroup2 has only UTE MRI, and ControlGroup3 has only CT.

considered statistically significant. To assess the agreement between CT and UTE MRI, Bland–Altman plots were generated. The mean of the normalized difference, the SD of the normalized difference, and the upper and lower limits of agreement (LOAs) were determined. Bias was estimated as the mean difference between the CT and MRI measurements for each measure, and Bland–Altman plots include corresponding 95% LOA. Extent of agreement was determined by whether the difference is significant or systematic bias exists in plots. Linear regressions were carried out for both CT and UTE MRI with EI as an outcome and FEV₁% predicted as a predictor.³¹ Correlation results based on linear regression analyses are reported as R², and a Fisher Z transformation was used to compare the strengths of the correlations. Confidence intervals for regression parameters related to FEV₁% predicted were computed to indicate agreement between those two measures in assessing EI.

Results

Table 1 displays subject demographic data for both COPD subjects and healthy controls. There was no significant differ-

ence in the average age, weight, or height between COPD and ControlGroup1 subjects. Representative axial CT and UTE MR images of a COPD subject and healthy control are displayed in Fig. 1. Despite the difference in lung inflation, near identical lung structures can be identified in both the CT and MR images. Little to no atelectasis formation was observed in the UTE MR images of either the control or COPD subjects. The average SNR measured in lung parenchyma from the UTE MR images of all subjects was 31.9 ± 10.8 (the SNR of COPD and controls subjects was 30.2 ± 9.4 and 33.5 ± 12.3, respectively). Figure 1 also displays representative examples of the segmentation method used for both CT and UTE MR images in the automated quantitative analysis of emphysematous lung. The average SNR measured in emphysematous lung (all thresholded voxels) from the UTE MR images of all subjects was 6.6 ± 2.7.

Regional lung analysis assessed the CT lung density and MR lung-signal density of gravitationally dependent

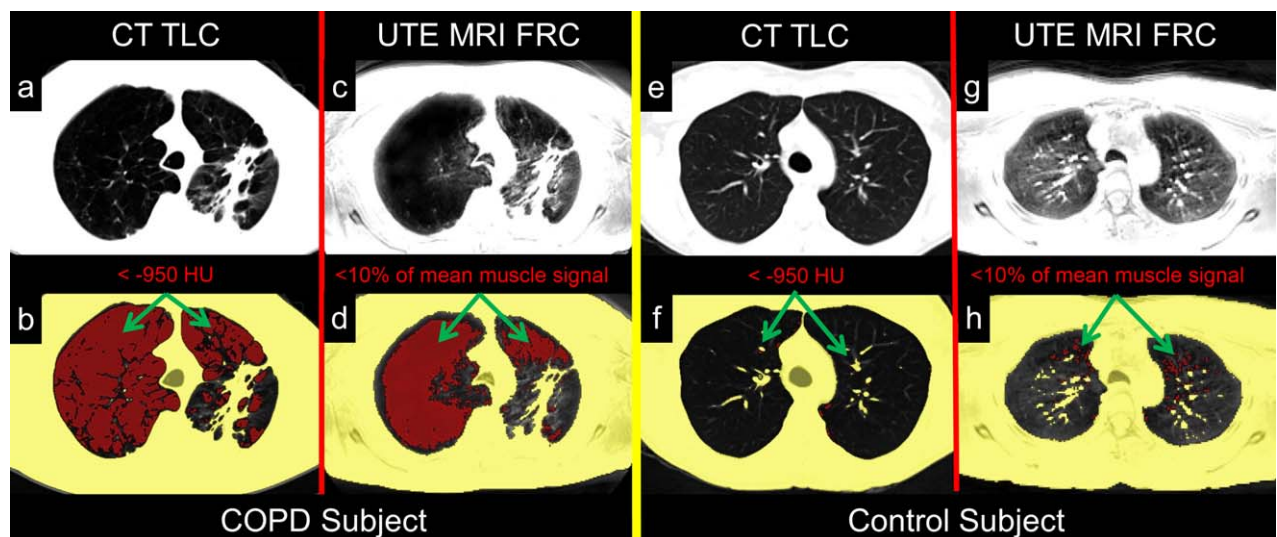


FIGURE 1: Displays the segmentation technique used on CT (a,b) and UTE MR (c,d) images of a COPD subject along with CT (e,f) and UTE MR (g,h) images of a healthy control subject. The segmented lower CT lung density and MR lung-signal density highlighted in the red mask is indicative of low density (emphysematous) lung.

TABLE 2. Subject Lung Analysis and PFT Results

Group	CT lung density	UTE MRI normalized lung-signal	CT EI (%)	UTE MRI EI (%)	FEV ₁ (%)
COPDs automated analysis	0.119 ± 0.031 n = 10	0.296 ± 0.067 n = 10	13.3 ± 14.9 n = 10	12.0 ± 9.8 n = 10	52.4 ± 24.6 n = 10
Controls automated analysis	0.149 ± 0.043 n = 18	0.390 ± 0.049 n = 10	0.23 ± 0.78 n = 18	2.40 ± 1.50 n = 10	102 ± 17.6 n = 19
COPD vs. Controls unpaired <i>t</i> -test (automated analysis)	0.043	0.0025	0.021	0.013	<0.0001
COPDs ROI analysis (paired <i>t</i> -test vs. automated analysis)	0.114 ± 0.028 n = 10 (<i>P</i> = 0.32)	0.277 ± 0.094 n = 10 (<i>P</i> = 0.15)	NA	NA	52.4 ± 24.6 n = 10
Controls ROI analysis (paired <i>t</i> -test vs. automated analysis)	0.139 ± 0.041 n = 18 (<i>P</i> < 0.0001)	0.405 ± 0.053 n = 10 (<i>P</i> = 0.35)	NA	NA	102 ± 17.6 n = 19
COPD vs. Controls unpaired <i>t</i> -test (ROI analysis)	0.057	0.002	NA	NA	<0.0001

(posterior ROI) and independent (anterior ROI) lung regions of the control subjects, with dependent regions having significantly greater density than the gravitationally independent regions (*P* < 0.001, both). There was no significant difference (*P* > 0.11) in lung density or signal density between the dependent and independent lung regions measured via CT or MRI of the COPD subjects. Regional lung analysis of CT images of the control subjects measured slightly lower lung densities (control 0.139 ± 0.039, COPD 0.114 ± 0.028) compared to the densities measured via the automated analysis of the whole-lung (control 0.149 ± 0.043 *P* = 0.0001, COPD 0.119 ± 0.031 *P* = 0.32), with slightly worse group differentiation (*P* = 0.057 vs. *P* = 0.043). For MR images there was no significant difference in signal densities measured via regional analysis (COPD 0.277 ± 0.094, Control 0.405 ± 0.053) compared to the signal densities measured via the whole-lung automated analysis (COPD 0.296 ± 0.067 *P* = 0.15, Control 0.390 ± 0.049 *P* = 0.35).

Results of the CT lung densities and MRI signal density and EI for both CT and UTE MRI are summarized in Table 2, along with FEV₁% predicted. The CT lung density and MR signal density quantified in the controls via CT and UTE MRI was 0.149 ± 0.043 and 0.390 ± 0.049, respectively; in the COPD subjects it was 0.119 ± 0.031 (*P* = 0.043) and 0.296 ± 0.067 (*P* = 0.0025), respectively. Figure 2 displays a moderate correlation (*R*² = 0.44, *P* <

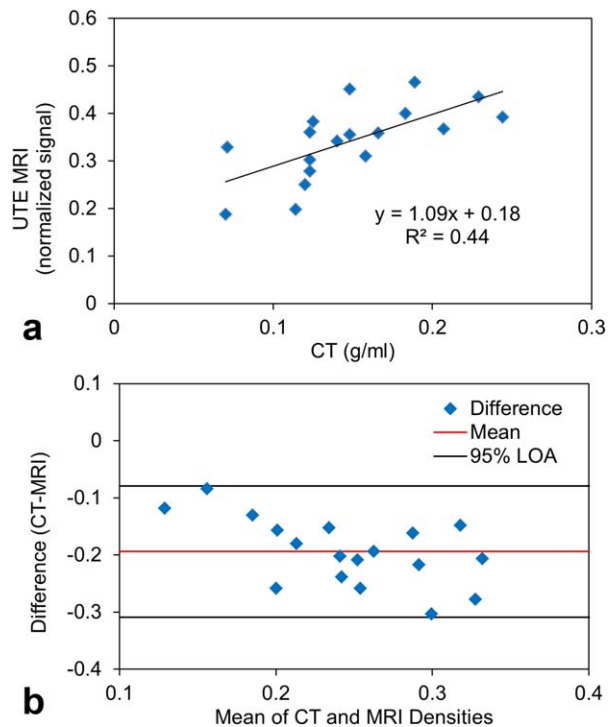


FIGURE 2: (a) UTE MRI lung-signal density plotted as a function of the CT lung density. (b) Bland-Altman plot of the agreement analysis of CT lung density and MR lung-signal density. Mean difference (CT, UTE MRI) = -0.19, 95% limits of agreement = -0.079 to -0.31.

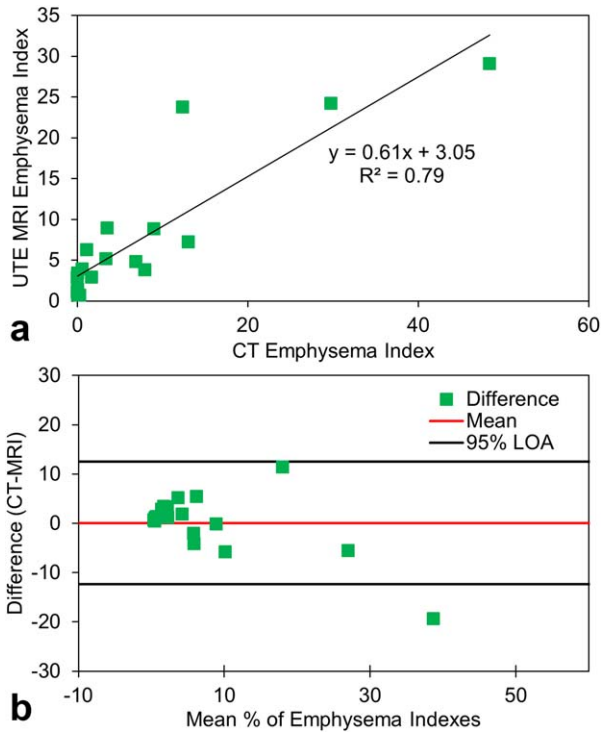


FIGURE 3: (a) CT EI plotted as a function of UTE MRI EI for subjects with both CT and UTE MR images. (b) Bland-Altman plot of the agreement analysis of emphysematous lung volume percentages for CT and UTE MRI. Mean difference (CT, UTE MRI) = 0.06, 95% limits of agreement = 12.50 to -12.38.

0.001) between the whole-lung signal density quantified from UTE MRI and the actual lung density determined from CT. The mean difference and 95% LOA for COPD subjects and healthy controls was -0.19 (-0.079 to -0.31). The EI quantified in controls via CT and UTE MRI was $0.23 \pm 0.78\%$ and $2.40 \pm 1.50\%$, respectively; in the COPD subjects it was $13.3 \pm 14.9\%$ ($P = 0.021$) and $12.0 \pm 9.8\%$ ($P = 0.013$), respectively. A nonparametric paired t -test ($P = 0.97$) determined that there was no difference between the EI quantified via UTE MRI and CT. Figure 3 displays a high correlation ($R^2 = 0.79$, $P < 0.0001$) between the EI determined from CT and UTE MR images. The mean difference and 95% LOA for COPD subjects and healthy controls was 0.06 (12.50 to -12.38).

There was not a significant elapsed timeframe ($P > 0.05$) between the date of the spirometry test and CT scan (11.3 ± 21.1 months) or MRI scan (0.57 ± 0.80 months). The FEV₁% predicted of each subject is plotted as a function of the EI determined by both CT and UTE MRI; these are displayed in Fig. 4. From linear regression analysis it was determined that there is moderate correlation between the decrease in FEV₁% predicted and the increase in both the UTE MRI EI ($R^2 = 0.65$, $P < 0.0001$) and CT EI ($R^2 = 0.49$, $P < 0.0001$). UTE MRI EI demonstrated a slightly higher correlation with FEV₁% predicted compared to CT EI; however, a Fisher Z transformation determined

that there was no significant difference in the strengths of these the correlations ($Z = 0.80$, $P = 0.42$). The overlapped confidence intervals for UTE MRI and CT were $(-0.34, -0.17)$ and $(-0.34, -0.15)$, respectively, which suggests agreement between both imaging modalities in assessing EI.

Discussion

Previous pulmonary UTE MRI studies have demonstrated correlation between CT lung density and MRI signal intensity measurements in COPD subjects.^{14,15} A recent study also assessed quality using the same scanner and sequence.¹³ The goal of this study was to further validate the ability of UTE MRI to quantify lung density and emphysema extent in subjects with COPD and illustrate its potential use as an imaging surrogate for CT. Importantly, we also sought to develop a quantitative UTE MRI emphysema index (EI) that is comparable to the well-validated CT emphysema index. Our UTE MRI protocol is sensitive to changes in lung density and is a viable candidate for evaluating emphysema both regionally and globally. Differences in lung density were visually apparent from subjects with varying degrees of emphysema. Despite the difference in lung inflation, near identical lung structures can be identified in the CT and MR images. Through our regional and automated quantitative analysis it was determined that there was a statistically significant and moderate correlation between the lung density quantified via CT and signal density quantified

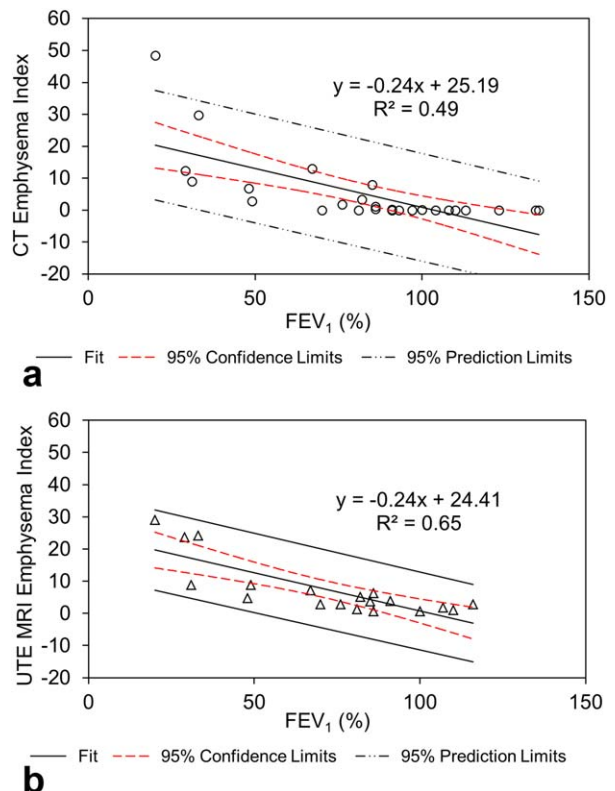


FIGURE 4: FEV₁% predicted plotted as a function of EI of (a) CT and (b) UTE MRI.

via UTE MR images of both the ControlGroup1 and COPD subjects. The measured CT lung density and MR signal density was lower in the COPD subjects compared to the controls. Regional lung analysis of CT lung density and MR signal density supports the results of our automated analysis of the whole lung. Furthermore, our automated quantitative analysis assessed the average lung and soft tissue signal over the entire volume imaged in order to minimize any spatial variations due to receiver coil sensitivity. We therefore believe that our quantification of signal density is quite robust, for any reasonable B_1 homogeneity in a typical coil used for chest imaging.

Based on the clinical CT EI routinely used for quantifying emphysema extent,^{27–29} we defined, in an attempt to generate an emphysema MRI biomarker, a similar index for UTE MR lung images. The threshold, fixed to <10% of the mean thoracic soft-tissue signal, proved to correlate well with the CT EI. Additional threshold values for UTE MR images were evaluated; however, the differences between the calculated CT EI and UTE MRI EI become more statistically significant above and below the 10% threshold. The question of precise sensitivity to early emphysema or change over time must be assessed in a subsequent longitudinal study. In this cross-sectional study there was a higher correlation between the FEV₁% predicted and UTE MRI EI compared to CT EI, but no significant difference between the strengths of these correlations. These results demonstrate that our UTE MRI protocol is able to assess emphysematous lung with strong correlation to CT and moderate correlation to FEV₁%.

UTE MRI acquisitions of the lung at 3T have previously demonstrated sensitivity to lung tissue density induced by lung inflation and gravity dependence.¹³ In this study, a similar imaging protocol including respiratory gating at FRC was used in order to yield heavily spin-density weighted lung images. The UTE MRI is acquired during free breathing and the RF excitation of the longitudinal magnetization and signal acquisition are limited to a gated acquisition window. One consequence of this gated acquisition is that a large portion of the longitudinal magnetization is recovered. The T_1 of the whole lung at 3T is around 1.4 seconds and with an effective repetition time of 3–4 seconds between subsequent triggering events; thus, during a typical breathing period, the recovered longitudinal magnetization between each gated acquisition is ~88% to 94%.³² Recent studies have determined that the T_1 of COPD lung tissue is significantly shorter (~950 msec at 1.5T) than that of healthy lung tissue (~1050 msec at 1.5T).^{33,34} Thus, the lung tissue of COPD patients is expected to recover additional longitudinal magnetization and have greater signal per alveolus compared to the controls. However, this is a small effect and in our study the signal in COPD was still well below control values. Although the echo time of this sequence is ultrashort compared to conventional MRI

sequences, there is a portion of transverse magnetization lost prior to signal acquisition. At 3T the T_2^* of the lungs is 0.74 msec; with an echo time of 0.17 msec this translates into a 21% decrease in the signal of the lungs compared to an echo time of zero.³⁵

One major difference between the CT and UTE MR images for all subjects is the lung volumes at which the images were acquired for each imaging modality. CT images were acquired during a static inspiratory breath-hold near total lung capacity (TLC). UTE MR images were acquired during a dynamic free-breathing session with gated acquisition at FRC. The difference in lung volume translates into a higher relative density of the lung parenchyma measured via the UTE MR images compared to CT. Additionally, as the UTE MR images were acquired at FRC, these images captured both emphysema and air trapping, and as such the UTE MR images are not a perfect comparison to the inspiratory CT images. Our threshold of 10% of the soft-tissue signal (corresponding to approximately -900 HU) reflects the lower lung volume and increased signal at FRC compared to TLC. Since this sequence is gated to capture lung-signal at FRC, the length of the scan depended on the individual subject's breathing pattern. The more irregular and variable breathing patterns became, the longer the scanning sessions became. In order to decrease scanning time for this validation study the volume of lung coverage (~160 mm in the through-plane) selected included the majority of the lungs, but sometimes clipped the most apical and basal sections of the lungs. This incomplete coverage of the lungs across all subjects did not adversely affect the quantification the MR lung-signal density or the implementation of an MRI-based EI. However, due to the heterogeneous nature of COPD, it is probable that a complete coverage of the lungs would lead to a more accurate quantification of EI in any individual patient.

Compared to conventional MRI, this UTE sequence captures more of the lung parenchyma signal; however, its resolution (0.72 pixels/mm) is comparatively lower than CT (1.28 pixels/mm). Another limitation of this study in assessing EI in COPD patients is that CT and MRI were acquired at different timepoints; average elapsed time between modalities was 9.4 ± 20 months. However, a recent study by Bhavani et al measured a +0.46% per year increase in EI in a cohort of COPD subjects.³⁶ Therefore, in these clinically stable patients we expect little to very mild progression of COPD severity in the time between modalities. In the case with particularly high EI, UTE MRI underestimates EI compared to CT, potentially as a result of some imperfect gating and motion of the chest wall. Future work will focus on continuous image acquisition in the steady-state regime during free breathing and implementing retrospective gating to separate inspiration from expiration.³⁷

In conclusion, this pilot study assessed our ability to generate and use an MRI-based EI in COPD patients. Previously, lung MRI has been envisioned as a complementary or alternative diagnostic approach to CT for lung disease in cases of increased tissue density and higher MRI signal intensity. This study demonstrates that UTE MRI can also be employed to quantify tissue losses in COPD patients via the EI, which is particularly useful in longitudinal studies and in patients who are vulnerable or sensitive to ionizing radiation. Furthermore, these results demonstrate that UTE MRI may serve as a biomarker for COPD extent and severity.

References

- Sverzellati N, Molinari F, Pirroni T, Bonomo L, Spagnolo P, Zompatori M. New insights on COPD imaging via CT and MRI. *Int J Chron Obstruct Pulmon Dis* 2007;2:301-312.
- Ley-Zaporozhan J, Ley S, Kauczor HU. Morphological and functional imaging in COPD with CT and MRI: present and future. *Eur Radiol* 2008;18:510-521.
- Smith-Bindman R, Miglioretti DL, Johnson E, et al. Use of diagnostic imaging studies and associated radiation exposure for patients enrolled in large integrated health care systems, 1996-2010. *JAMA* 2012;307:2400-2409.
- de Jong PA, Mayo JR, Golmohammadi K, et al. Estimation of cancer mortality associated with repetitive computed tomography scanning. *Am J Respir Crit Care Med* 2006;173:199-203.
- Bergin CJ, Noll DC, Pauly JM, Glover GH, Macovski A. MR imaging of lung parenchyma: a solution to susceptibility. *Radiology* 1992;183:673-676.
- Kauczor HU, Kreitner KF. MRI of the pulmonary parenchyma. *Eur Radiol* 1999;9:1755-1764.
- Mayo JR, MacKay A, Müller NL. MR imaging of the lungs: value of short TE spin-echo pulse sequences. *AJR Am J Roentgenol* 1992;159:951-956.
- Bergin CJ, Pauly JM, Macovski A. Lung parenchyma: projection reconstruction MR imaging. *Radiology* 1991;179:777-781.
- Johnson KM, Fain SB, Schiebler ML, Nagle S. Optimized 3D ultrashort echo time pulmonary MRI. *Magn Reson Med* 2013;70:1241-1250.
- Bauman G, Puderbach M, Deimling M, et al. Non-contrast-enhanced perfusion and ventilation assessment of the human lung by means of Fourier decomposition in proton MRI. *Magn Reson Med* 2009;62:656-664.
- Bauman G, Lützen U, Ullrich M, et al. Pulmonary functional imaging: qualitative comparison of Fourier decomposition MR imaging with SPECT/CT in porcine lung. *Radiology* 2011;260:551-559.
- Togao O, Tsuji R, Ohno Y, Dimitrov I, Takahashi M. Ultrashort echo time (UTE) MRI of the lung: assessment of tissue density in the lung parenchyma. *Magn Reson Med* 2010;64:1491-1498.
- Lederlin M, Crémillieux Y. Three-dimensional assessment of lung tissue density using a clinical ultrashort echo time at 3 Tesla: a feasibility study in healthy subjects. *J Magn Reson Imaging* 2014;40:839-847.
- Ma W, Sheikh K, Svenningsen S, et al. Ultra-short echo-time pulmonary MRI: evaluation and reproducibility in COPD subjects with and without bronchiectasis. *J Magn Reson Imaging* 2015;41:1465-1474.
- Ohno Y, Koyama H, Yoshikawa T, et al. T2* measurements of 3-T MRI with ultrashort TEs: capabilities of pulmonary function assessment and clinical stage classification in smokers. *AJR Am J Roentgenol* 2011;197:W279-285.
- Togao O, Tsuji R, Ohno Y, Dimitrov I, Takahashi M. Ultrashort echo time (UTE) MRI of the lung: assessment of tissue density in the lung parenchyma. *Magn Reson Med* 2010;64:1491-1498.
- Takahashi M, Togao O, Obara M, et al. Ultra-short echo time (UTE) MR imaging of the lung: comparison between normal and emphysematous lungs in mutant mice. *J Magn Reson Imaging* 2010;32:326-333.
- Zurek M, Boyer L, Caramelle P, Boczkowski J, Crémillieux Y. Longitudinal and noninvasive assessment of emphysema evolution in a murine model using proton MRI. *Magn Reson Med* 2012;68:898-904.
- Lederlin M, Bauman G, Eichinger M, et al. Functional MRI using Fourier decomposition of lung signal: reproducibility of ventilation- and perfusion-weighted imaging in healthy volunteers. *Eur J Radiol* 2013;82:1015-1022.
- Bauman G, Puderbach M, Heimann T, et al. Validation of Fourier decomposition MRI with dynamic contrast-enhanced MRI using visual and automated scoring of pulmonary perfusion in young cystic fibrosis patients. *Eur J Radiol* 2013;82:2371-2377.
- Schönfeld C, Cebotari S, Voskrebenez A, et al. Performance of perfusion-weighted Fourier decomposition MRI for detection of chronic pulmonary emboli. *J Magn Reson Imaging* 2015;42:72-79.
- Qing K, Ruppert K, Jiang Y, et al. Regional mapping of gas uptake by blood and tissue in the human lung using hyperpolarized xenon-129 MRI. *J Magn Reson Imaging* 2014;39:346-359.
- Thomen RP, Sheshadri A, Quirk JD, et al. Regional ventilation changes in severe asthma after bronchial thermoplasty with (3)He MR imaging and CT. *Radiology* 2015;274:250-259.
- Quirk JD, Lutey BA, Gierada DS, et al. In vivo detection of acinar microstructural changes in early emphysema with (3)He lung morphometry. *Radiology* 2011;260:866-874.
- Kirby M, Ouriadov A, Svenningsen S, et al. Hyperpolarized 3He and 129Xe magnetic resonance imaging apparent diffusion coefficients: physiological relevance in older never- and ex-smokers. *Physiol Rep* 2014;2(7).
- Walkup LL, Woods JC. Translational applications of hyperpolarized 3He and 129Xe. *NMR Biomed* 2014;27:1429-1438.
- Gevenois PA, Scillia P, de Maertelaer V, Michils A, De Vuyst P, Yemault JC. The effects of age, sex, lung size, and hyperinflation on CT lung densitometry. *AJR Am J Roentgenol* 1996;167:1169-1173.
- Parr DG, Stoel BC, Stolk J, Nightingale PG, Stockley RA. Influence of calibration on densitometric studies of emphysema progression using computed tomography. *Am J Respir Crit Care Med* 2004;170:883-890.
- Gierada DS, Bierhals AJ, Choong CK, et al. Effects of CT section thickness and reconstruction kernel on emphysema quantification relationship to the magnitude of the CT emphysema index. *Acad Radiol* 2010;17:146-156.
- Vestbo J, Hurd SS, Agustí AG, et al. Global strategy for the diagnosis, management, and prevention of chronic obstructive pulmonary disease: GOLD executive summary. *Am J Respir Crit Care Med* 2013;187:347-365.
- Bland JM, Altman DJ. Regression analysis. *Lancet* 1986;1:908-909.
- Nichols MB, Paschal CB. Measurement of longitudinal (T1) relaxation in the human lung at 3.0 Tesla with tissue-based and regional gradient analyses. *J Magn Reson Imaging* 2008;27:224-228.
- Alamidi DF, Kindvall SS, Hubbard Cristinacce PL, et al. T1 relaxation time in lungs of asymptomatic smokers. *PLoS One* 2016;11:e0149760.
- Alamidi DF, Morgan AR, Hubbard Cristinacce PL, et al. COPD patients have short lung magnetic resonance T1 relaxation time. *COPD* 2016;13:153-159.
- Yu J, Xue Y, Song HK. Comparison of lung T2* during free-breathing at 1.5T and 3.0 T with ultrashort echo time imaging. *Magn Reson Med* 2011;66:248-254.
- Bhavani S, Tsai CL, Perusich S, et al. Clinical and immunological factors in emphysema progression. Five-year prospective longitudinal exacerbation study of chronic obstructive pulmonary disease (LES-COPD). *Am J Respir Crit Care Med* 2015;192:1171-1178.
- Higano NS, Hahn AD, Tkach JA, et al. Retrospective respiratory self-gating and removal of bulk motion in pulmonary UTE MRI of neonates and adults. *Magn Reson Med* 2016 [Epub ahead of print].